Interfacial coupling effect of Cr_2O_3 on the magnetic properties of $Fe_{72}Ga_{28}$ thin films

I. Hontecillas
Universidad Complutense de Madrid
M. Maicas
Polytechnic University of Madrid (UPM)
J. P. Andrés
University of Castile-La Mancha
R. Ranchal (rociran@ucm.es)
Universidad Complutense de Madrid

Research Article

Keywords: perpendicular magnetic anisotropy, stripe domains, exchange-bias

Posted Date: April 9th, 2021

DOI: https://doi.org/10.21203/rs.3.rs-398847/v1

Abstract

Here it is investigated the effect of the antiferromagnet Cr_2O_3 on the magnetic properties of ferromagnetic $Fe_{72}Ga_{28}$ thin films. Although $Fe_{72}Ga_{28}$ layers have their magnetization almost in the sample plane, the interfacial coupling with Cr_2O_3 that has perpendicular magnetic moments enables to turn the $Fe_{72}Ga_{28}$ magnetization direction into the out of plane (OOP) direction. Cr_2O_3 has been obtained from Cr oxidation, whereas $Fe_{72}Ga_{28}$ has been deposited on top of it by sputtering in the ballistic regime. Although a uniaxial in-plane magnetic anisotropy is expected for $Fe_{72}Ga_{28}$ thickness above 100 nm, the interfacial coupling with Cr_2O_3 prevents this anisotropy. The formation of stripe domains in $Fe_{72}Ga_{28}$ above a critical thickness reveals the enhancement of the out of plane component of the $Fe_{72}Ga_{28}$ magnetization with respect to uncoupled layers. Due to the interface coupling, the $Fe_{72}Ga_{28}$ magnetization turns into the out-of-plane direction as its thickness is gradually reduced, and a perpendicular magnetic anisotropy of $3.4{\cdot}10^6$ erg·cm^{-3} is inferred from experimental results. Eventually, the coupling between Cr_2O_3 and $Fe_{72}Ga_{28}$ promotes an exchange-bias effect that has been well fitted by means of the random field model.

1. Introduction

Control of the magnetization is an important issue for the development of pioneering magnetic devices. Typically, thin films have the magnetization in the sample plane in order to reduce the energy of the system [1]. However, in many applications as for example: high density magnetic storage, spintronic devices, non-volatile random access memories, logic devices, skyrmions or sensors, materials with OOP magnetization are desirable [2–6].

Systems with large perpendicular magnetic anisotropy (PMA) such as $L1_0$ FePt and CoPt thin films are extensively investigated but, their large coercivity and switching fields can represent a drawback for their integration in devices [7–8]. Therefore, it is of interest the investigation of other materials with PMA, or the possibility of turning the magnetization into the OOP direction. Stripe domains appear above a critical thickness when a moderate PMA is present [9]. In permalloy films, stripes have been observed because of columnar growth [10], but they have also been promoted when coupled with NdCo [11]. Recently, the magnetization direction has been tuned in Fe-N layers by ion implantation and heat treatment conditions [9], and by annealing in $Fe_{87}Si_9B_{13}$ [12]. Even more notably, the control of the magnetic anisotropy by means of voltage has been observed at magnetic transition metal/oxide interfaces [2].

FeGa alloys are extensively studied because of their large magnetostriction constant and low coercivity [13–16]. Also interesting is the possibility in sputtered $Fe_{72}Ga_{28}$ layers of controlling the in-plane magnetic anisotropy by growth conditions [17–19] or by thermal treatments combined with mechanical stress [20]. Molecular beam epitaxy (MBE) FeGa can exhibit domain stripes due to a low PMA [21–23], but the general behavior observed by MFM in FeGa deposited either by electrodeposition [24], sputtering

[25] or even MBE [26] is a magnetic ripple due to magnetic fluctuations with the magnetization almost in the sample plane.

In this work, we have explored the possibility of turning the $Fe_{72}Ga_{28}$ magnetization into the OOP direction when appropriately coupled with the Cr_2O_3, an antiferromagnet that has its magnetic moments in the perpendicular direction [27–29]. Although Cr_2O_3 has already been coupled with ferromagnetic metals [30–32], the interaction with $Fe_{72}Ga_{28}$ seems not a trivial problem. $Fe_{72}Ga_{28}$ has already been coupled with $TbFe_2$ in [$Fe_{72}Ga_{28}$/$TbFe_2$] multilayers to turn its magnetization into the OOP direction [33–34]. However, only a tilt of the magnetization of around 25° with respect to the sample plane was achieved despite the large PMA of $TbFe_2$ [33–34]. Here we show that thanks to an appropriate election of layer thickness and coupling material, it is possible to reach an effective interfacial interaction that enables to turn the $Fe_{72}Ga_{28}$ magnetization into the OOP direction. In addition, thanks to the interfacial interaction we have observed exchange-bias effect in the perpendicular direction being possible to fit the experimental exchange-bias fields (H_E) by means of the random field model [35–37].

2. Experimental Section

30 nm-thick Cr_2O_3 was synthetized from the evaporation of Cr on glass substrates that was subsequently oxidized in oxygen atmosphere at 750 °C during 3 hours. $Fe_{72}Ga_{28}$ layers with a thickness ranging from 240 to 20 nm were grown by the DC magnetron sputtering technique in the ballistic regime at room temperature on top of the Cr_2O_3. The sputtering deposition was carried out in oblique incidence with an angle between the vapor beam and the perpendicular to the sample of about 25° and a distance of 9 cm between target and substrate. This direction of the vapor beam within the sample plane is taken as the reference direction to control the direction of the in-plane uniaxial anisotropy axis when created [16–17, 38]. $Fe_{72}Ga_{28}$ films were deposited from a target with a composition of $Fe_{72}Ga_{28}$ with a diameter of 5 cm and a thickness of 2 mm using an Ar pressure of $3{\cdot}10^{-3}$ mbar and a growth power of 90 W in all cases. A 20-nm thick Mo layer was used as a capping layer to avoid FeGa oxidation. Mo was also deposited with a power of 90 W and with an Ar pressure of $3{\cdot}10^{-3}$ mbar. Therefore, the structure of the studied samples is: glass/ Cr_2O_3/$Fe_{72}Ga_{28}$/Mo.

We have used X-ray diffractometry (XRD) in the Bragg-Brentano configuration to study the structural properties. Measurements were performed in a Philips X'Pert MPD using the Cu K_α wavelength (1.54056 Å). A Digital Instruments Nanoscope IIIa instrument was used to obtain Magnetic Force Microscopy (MFM) images. We monitored the cantilever's phase of oscillation while the magnetic tip was scanning the sample surface to work in the phase detection mode. The distance between sample and surface was 40 nm on average (lift mode) [33]. The MFM measurements were performed without magnetic field after an OOP magnetic field of 10 kOe was applied. In-plane and OOP hysteresis loops were performed in a vibrating sample magnetometer (VSM) at room temperature. In the sample plane, we measured loops at different angles between the applied magnetic field and the in-plane reference direction. As a reference

dence direction in the sample plane [17, 38]. Hysteresis loops

at 5 K were measured in a SQUID magnetometer after a field-cooling process (FC) at 1 kOe from 360 K. In this case, only OOP loops were recorded.

3. Results And Discussion

First of all, we have analyzed the possibility of $Fe_{72}Ga_{28}$ oxidation because of its growth on top of Cr_2O_3 (Fig. 1). XRD measurements do not show evidences of oxidation within the resolution technique. The diffraction patterns are similar to what we have previously reported about sputtered $Fe_{72}Ga_{28}$ being the (110) the main $Fe_{72}Ga_{28}$ diffraction peak [16–19]. On the other hand, the diffraction peaks of Cr_2O_3 show no variations upon the deposition of $Fe_{72}Ga_{28}$ on top of it (Fig. 1).

Sputtered $Fe_{72}Ga_{28}$ layers deposited in the ballistic regime develop in-plane magnetic anisotropy above 100 nm [16, 18]. Nevertheless, the coupling with Cr_2O_3 completely eliminate this in-plane anisotropy even for thicknesses well above 100 nm (Fig. 2a). This can be understood considering that a sample will show PMA if two conditions are fulfilled: i) it is magnetically isotropic in the sample plane, and ii) the OOP direction is an easy axis in comparison to any direction in the sample plane. Therefore, the absence of in-plane magnetic anisotropy is a necessary condition for the PMA to be developed.

The VSM hysteresis loops also reveal the change of the magnetization direction from in-plane to OOP as the $Fe_{72}Ga_{28}$ thickness is reduced (Fig. 2b). We can quantitively monitor this evolution by means of the OOP squareness (M_r/M_{max}) defined as the ratio between the remanence (M_r) and the maximum magnetization (M_{max}) obtained in the perpendicular hysteresis loops. In table 1 we can observe how the squareness increases as the $Fe_{72}Ga_{28}$ thickness is reduced, mostly for a thickness below 80 nm.

MFM images can also be used to monitor the influence of the Cr_2O_3 on the $Fe_{72}Ga_{28}$ magnetic behavior (Fig. 3). When $Fe_{72}Ga_{28}$ is no coupled (Fig. 3a), it is observed the magnetic contrast known as magnetic ripple in agreement with previous works [24–26]. However, due to the interfacial coupling with Cr_2O_3, the OOP component of the magnetization of $Fe_{72}Ga_{28}$ is enhanced, and stripe domains start to be visible in the MFM images (Fig. 3b-d).

In ferromagnetic materials with PMA, the quality factor Q is defined as:

$$Q = K_{FM}/2\pi M_{FM}^2$$

1

where K_{FM} is the perpendicular magnetic anisotropy, and M_{FM} is the magnetization saturation [9, 39]. For materials with moderate or low PMA, $Q < 1$, and stripe domains appear above a critical thickness (t_{cr}):

$$t_{cr} = 2\pi\sqrt{A_{ex}/K_{FM}}$$

where A_{ex} is the exchange energy per unit length. When $Q > 0.1$, stripe domains are wider than the layer thickness, whereas they exhibit a periodicity equals to the layer thickness if $Q < 0.1$.

We have inferred K_{FM} from the comparison of in-plane and OOP hysteresis loops following the work of Garnier *et al*. [9]. In average, we have obtained a K_{FM} of $3.4 \cdot 10^6$ erg/cm^3. Taking M_{FM} as 1100 emu·cm^{-3} [26], it is inferred a Q of 0.3 in our samples and therefore, stripes are expected above a critical thickness. Considering $A_{ex} = 1.7 \cdot 10^{-6}$ erg·cm^{-1} from the literature [22–23, 40], and using Eq. (2), it is obtained an experimental t_{cr} of 44 nm. This is in agreement with our experimental findings in which stripes have only been observed for $Fe_{72}Ga_{28}$ thickness ≥ 40 nm. In fact, if we take this experimental value as t_{cr}, a K_{FM} of $4 \cdot 10^6$ erg·cm^{-3} is calculated, pretty close to the value inferred from experimental hysteresis loops. Finally, from the MFM images we have obtained a stripe period of 125 nm by means of the power spectral density. This stripe periodicity higher than the layer thickness is consistent with the quality factor Q higher than 0.1 calculated in our samples.

In addition to the rotation of the $Fe_{72}Ga_{28}$ direction magnetization towards the perpendicular direction, we have observed an exchange-bias effect related to the Cr_2O_3/ $Fe_{72}Ga_{28}$ interfacial coupling as indicated by the shift of the hysteresis loop in the horizontal axis (H_E) at 5 K after a FC process at 1 kOe (Fig. 4). This exchange-bias phenomenon in the perpendicular direction is related to the exchange-coupling between the antiferromagnetic Cr_2O_3, and the ferromagnetic $Fe_{72}Ga_{28}$ [41]. For a $Fe_{72}Ga_{28}$ thickness of 20 nm, H_E is -17 Oe, and -9 Oe for a thickness of 40 nm.

Since the perpendicular magnetic anisotropy inferred in this work for $Fe_{72}Ga_{28}$ ($K_{FM} = 3.4 \cdot 10^6$ erg·cm^{-3}) is higher than the theoretical value of Cr_2O_3 ($K_{AF} = 2 \cdot 10^5$ erg·cm^{-3}) [42], and some chemical roughness is expected at the $Fe_{72}Ga_{28}/Cr_2O_3$ interface, we have used the random field model proposed by Malozemoff [35–37] to calculate the theoretical H_E values. In this random field model, the AF layer breaks into domains, and the exchange-bias field is obtained thanks to the expression:

$$H_E = \frac{2z\sqrt{A_{AF}K_{AF}}}{\pi^2 M_{FM} t_{FM}} \quad (3)$$

where z is generally taken as the unity, and A_{AF} is the exchange stiffness of the antiferromagnet that takes a value of $4 \cdot 10^7$ erg/cm [42]. With this expression (3) we obtain H_E equals to -26 Oe and − 13 Oe for $Fe_{72}Ga_{28}$ thickness of 20 and 40 nm, respectively, that are pretty close to the experimental − 17 Oe and − 9 Oe, respectively. This well agreement confirms the possibility of using this model in Cr_2O_3-based exchange-biased systems as also previously reported [42].

Finally, from H_E experimental values the interfacial exchange energy ΔE can be calculated:

$$\Delta E = H_E 2 M_{FM} t_{FM}$$

4

For $Fe_{72}Ga_{28}$ of 20 nm and 40 nm, it is obtained a ΔE of 0.08 erg·cm^{-2} that is higher than in previous works in which Cr_2O_3 has been coupled with other ferromagnets with reported values of 0.05 erg·cm^{-2} at 5 K [30, 41].

4. Conclusions

In summary, we have studied the effect of the interfacial coupling between an antiferromagnet with perpendicular magnetic moments (Cr_2O_3) and a ferromagnet ($Fe_{72}Ga_{28}$) with the magnetization almost in the sample plane. First of all, the in-plane magnetic anisotropy of $Fe_{72}Ga_{28}$ is completely vanished due to the coupling. Secondly, stripe domains are promoted due to the enhancement of the OOP component of the $Fe_{72}Ga_{28}$ magnetization. We have observed that the magnetization direction of $Fe_{72}Ga_{28}$ is gradually turned from in-plane to the OOP direction as the $Fe_{72}Ga_{28}$ thickness is reduced A perpendicular magnetic anisotropy of $3.4 \cdot 10^6$ erg·cm^{-3} has been inferred from experimental results in the $Fe_{72}Ga_{28}$ layers. It has also been observed exchange-bias phenomena in the perpendicular direction fitting the experimental data to the random field model.

Declarations

Acknowledgements.

“CAI Difracción Rayos-X” from UCM is also acknowledged for XRD measurements. This work has been financially supported through the projects RTI2018-097895-B-C43 of the Spanish Ministry of Science, Innovation, and Universities and MAT2017-87072-C4-3-P of the Spanish Ministry of Economy, Industry and Competitiveness.

The data that support the findings of this study are available from the corresponding author upon reasonable request.

References

1. Chikazumi, S. Physics of ferromagnetism. Oxford Science Publications(1997).
2. Fert, A., Reyren, A. N. & Cros, V. *Nat. Rev. Mater.* **2**, 17031 (2017).
3. Dieny, B. & Chshiev, M. *Rev. Mod. Phys.* **89**, 025008 (2017).
4. Sbiaa, R., Meng, H. & Piramanayagam, S. N. *Phys. Status Solidi RRL.* **5**, 413 (2011).
5. Umadevi, K., Bysakh, S., Arout Chelvane, J., Kamat, S. V. & Jayalaskhmi, V. *J. Alloys Compnd.* **663**, 430 (2016).

50, 363001 (2017).

7. Sbiaa, R., Law, R., Tan, E. L. & Liew, T. *J. Appl. Phys.* **105**, 013910 (2009).
8. Krivorotov, I. N. *et al. Science.* **307**, 228 (2005).
9. Garnier, L. C. *et al. J. Phys. Mater.* **3**, 024001 (2020).
10. Romera, M., Ranchal, R., Ciudad, D., Maicas, M. & Aroca, C. *J. Appl. Phys.* **110**, 083910 (2011).
11. Markó, D. *et al.* L. M. Álvarez-Prado, Appl. Phys. Lett. 115, 082401(2019).
12. Coïsson, M., Barrera, G. & Celegato, F. *and P. Tiberto Appl. Surf. Sci.* **476**, 402 (2019).
13. Ranchal, R. & Maestre, D. *J. Phys. D: Appl. Phys.* **47**, 355004 (2014).
14. Clark, A. E., Restorff, J. B., Wun-Fogle, M., Lograsso, T. A. & Schlagel, D. L. *IEEE Trans. Magn.* **36**, 3238 (2000).
15. Clark, A. E., Wun-Fogle, M., Lograsso, T. A. & Cullen, J. R. *IEEE Trans. Magn.* **37**, 2678 (2001).
16. Bartolomé, P., Begué, A., Muñoz-Noval, A., Ciria, M. & Ranchal, R. *J. Phys. Chem. C.* **124**, 4717 (2020).
17. Muñoz-Noval, A., Ordóñez-Fontes, A. & Ranchal, R.Phys. Rev. B**93**,214408, (2016).
18. Muñoz-Noval, A., Fin, S., Salas-Colera, E., Bisero, D. & Ranchal, R. *J. Alloys Compnd.* **745**, 413 (2018).
19. Muñoz-Noval, A., Salas-Colera, E. & Ranchal, R. *J. Phys. Chem. C.* **123**, 13131 (2019).
20. Hontecillas, I., Figueruelo, I., Abad, S. & Ranchal, R. *J. Magn. Magn. Mater.* **494**, 165771 (2020).
21. Barturen, M. *et al. Appl. Phys. Lett.* **101**, 092404 (2012).
22. Tacchi, S. *et al. Phys. Rev. B.* **89**, 024411 (2014).
23. Fin, S. *et al. Phys. Rev. B.* **92**, 224411 (2015).
24. Ranchal, R., Fin, S. & Bisero, D. *J. Phys. D: Appl. Phys.* **48**, 075001 (2015).
25. Bartolomé, P., Maicas, M. & Ranchal, R. *J. Magn. Magn. Mater.* **514**, 167183 (2020).
26. Begué, A., Proiettia, M. G., Arnaudas, J. I. & Ciria, M. *J. Magn. Magn. Mater.* **498**, 166135 (2020).
27. Kosub, T. *et al. Nat. Comm.* **8**, 13985 (2017).
28. Fallarino, L., Binek, C. & Berger, A. *Phys. Rev. B.* **91**, 214403 (2015).
29. He, X. *et al. Nat. Mater.* **9**, 579 (2010).
30. Lin, K. W. & Guo, J. Y. *J. Appl. Phys.* **104**, 123913 (2008).
31. Yuan, W. *et al. Sci. Rep.* **6**, 28397 (2016).
32. Nozaki, T. *et al. Appl. Phys. Lett.* **105**, 212406 (2014).
33. Bartolomé, P., Maicas, M., Biskup, N., Varela, M. & Ranchal, R. *Phys. Status Solidi A.* **215**, 1800183 (2018).
34. Bartolomé, P. & Ranchal, R. *Nanotechn.* **31**, 335715 (2020).
35. Malozemoff, A. P. *Phys. Rev. B.* **35**, 3679 (1987).
36. Malozemoff, A. P. *J. Appl. Phys.* **63**, 3874 (1988).
37. A. P.Malozemoff. Phys. Rev. B**37**,7673(1988).
38. Maicas, M., Ranchal, R., Aroca, C., Sánchez, P. & López, E. *Eur. Phys. J. B.* **62**, 267 (2008).

39. Hubert, A. & Schäfer, R. Magnetic domains: the analysis of magnetic microstructures, Springer Science & Business Media(2008).
40. Gopman, D. B., Sampath, V., Ahmad, H., Bandyopadhyay, S. & Atulasimha, J. *IEEE Trans. Magn.* **53**, 6101304 (2017).
41. Nogués, J. & Schuller, I. K. *J. Magn. Magn. Mater.* **192**, 203 (1999).
42. Zheng, R. K., Liu, H., Wang, Y. & Zhang, X. X. *Appl. Phys. Lett.* **84**, 702 (2004).

Table

Table 1. Summary of the OOP squareness (M_r/M_{max}) calculated from the perpendicular hysteresis loops as a function of the $Fe_{72}Ga_{28}$ thickness.

$Fe_{72}Ga_{28}$ thickness (nm)	**20**	**40**	**80**	**160**	**240**
M_r/M_{max} (OOP direction)	0.5	0.3	0.2	0.2	0.2

Figures

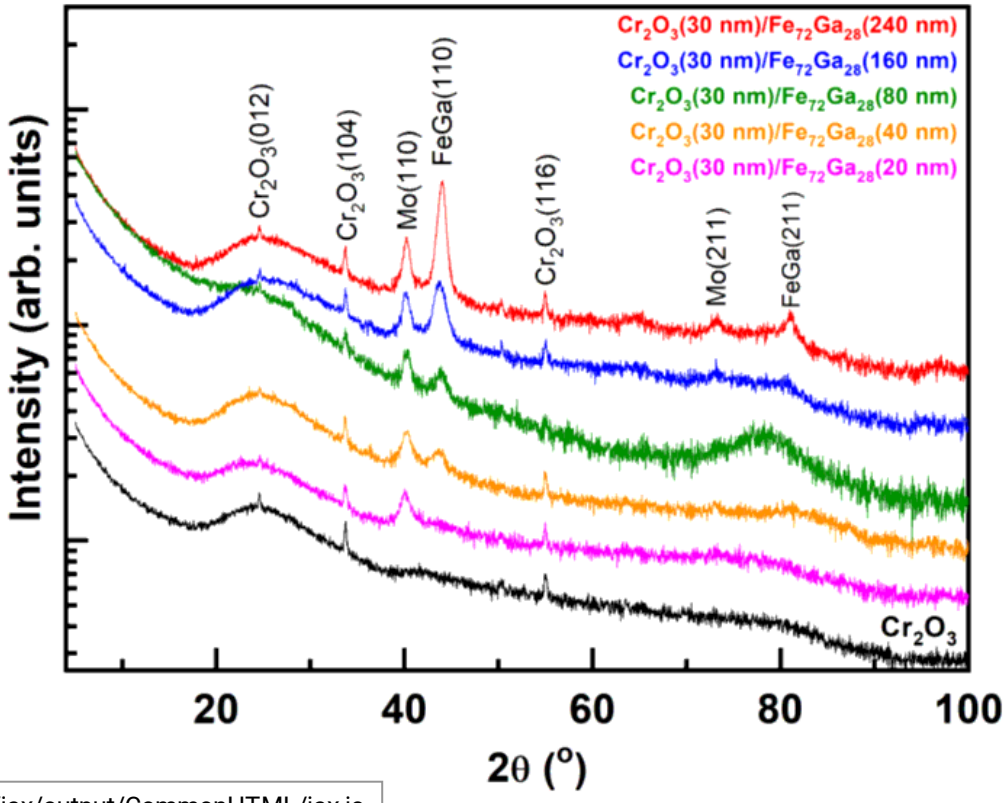

Figure 1

XRD diffraction patterns of the samples studied in this work. The measurement for a 30 nm-thick Cr2O3 layer on glass has been included for further comparisons. Curves are shifted for clarity.

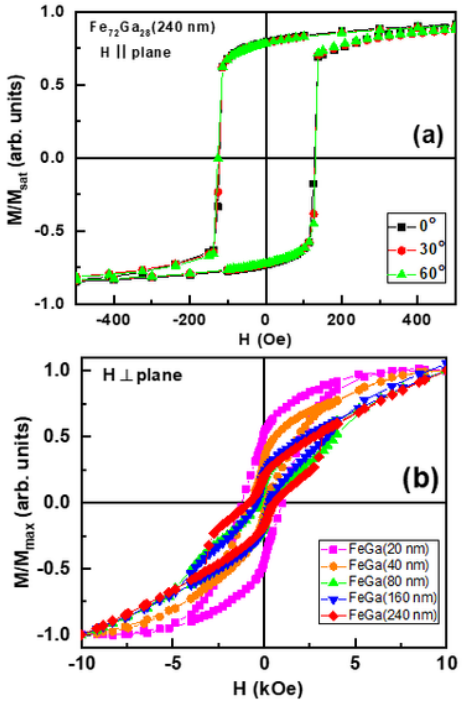

Figure 2

(a) In-plane room temperature hysteresis loops recorded for different angles between the reference direction taken as the reference beam direction and the applied magnetic field (■) 0°, (●) 30°, and (▲) 60°. (b) OOP hysteresis loops recorded at room temperature for samples with different FeGa thickness (■) 20 nm, (●) 40 nm, (▲) 80 nm, (▼) 160 nm, and (♦) 240 nm.

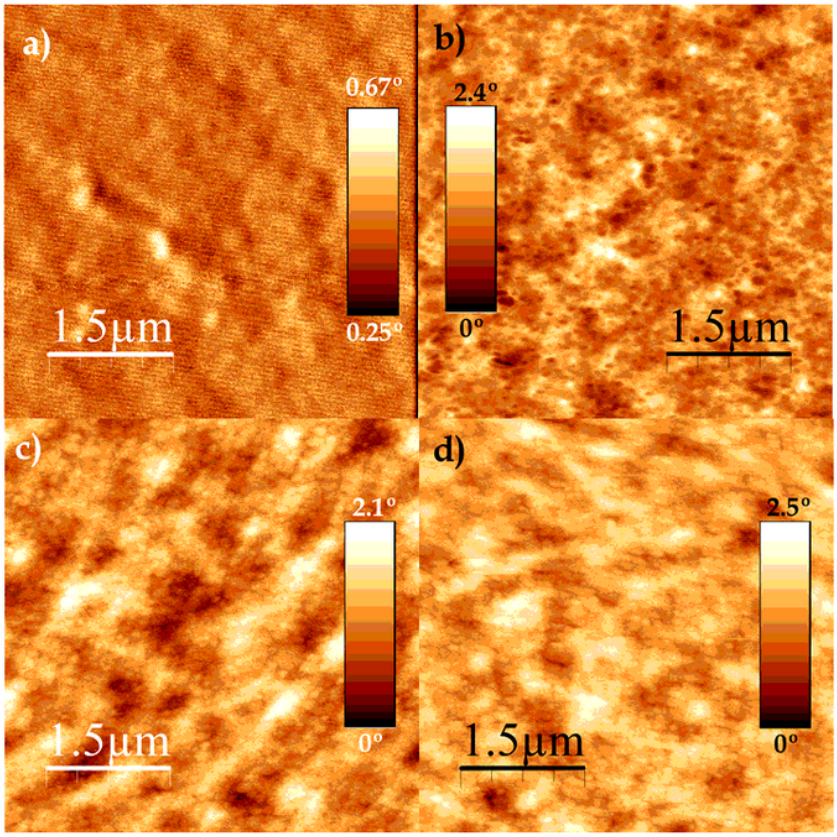

Figure 3

MFM images taken at remanence after an applied magnetic field of 10 kOe was applied in the perpendicular direction. (a) 150 nm-thick uncoupled Fe72Ga28 layer, (b) Cr2O3/Fe72Ga28(160 nm), (c) Cr2O3/Fe72Ga28(80 nm), and (d) Cr2O3/Fe72Ga28(40 nm).

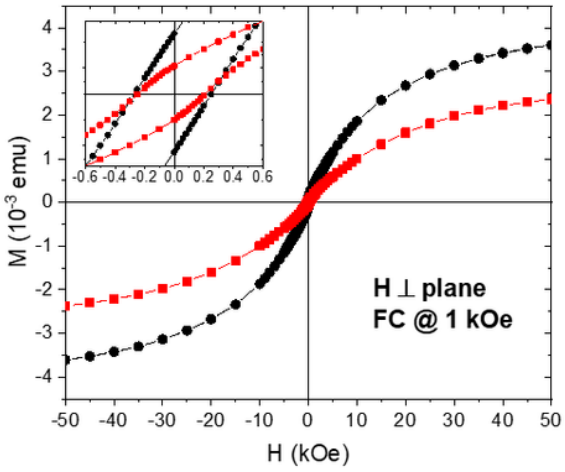

Figure 4

OOP hysteresis loops recorded at 5 K after FC at 1 kOe from 360K for samples with a FeGa thickness of (■) 20 nm, (●) 40 nm. Inset shows the low-field region.